# Remote Sensing and Machine Learning for Riparian Vegetation Detection and Classification

Nicholas Fiorentini
*National Research Council (CNR)*
*University of Pisa*
Pisa, Italy
0000-0002-8769-8610

Manlio Bacco
*National Research Council (CNR)*
Pisa, Italy
0000-0001-6733-1873

Alessio Ferrari
*National Research Council (CNR)*
Pisa, Italy
0000-0002-0636-5663

Massimo Rovai
*University of Pisa*
Pisa, Italy
0000-0001-5970-9223

Gianluca Brunori
*University of Pisa*
Pisa, Italy
0000-0003-2905-9738

***Abstract*—Precise and reliable identification of riparian vegetation along rivers is of paramount importance for managing bodies, enabling them to accurately plan key duties, such as the design of river maintenance interventions. Nonetheless, manual mapping is significantly expensive in terms of time and human costs, especially when authorities have to manage extensive river networks. Accordingly, in the present paper, we propose a methodology for detecting and automatically classifying the riparian vegetation of urban rivers. Specifically, the calibration of an unsupervised (Isodata Clustering) and a supervised (Random Forest) machine learning algorithm (MLA) is carried out for the classification of the riparian vegetation detected in aerial orthoimages with a resolution of 1 meter. Riparian vegetation is classified using Normalized Difference Vegetation Index (NDVI) features. In the framework of this research, the Isodata Clustering slightly outperforms the Random Forest, achieving a higher level of predictive performance and reliability throughout all the computed performance metrics. Moreover, being unsupervised, it does not require ground truth information, which makes it particularly competitive in terms of annotation costs when compared with supervised algorithms, and definitely appropriate in case of limited resources. We encourage river authorities to use MLA-based tools, such as the ones we propose in this work, for mapping riparian vegetation, since they can bring relevant benefits, such as limited implementation costs, easy calibration, fast training, and adequate reliability.**

***Index Terms*—Automatic Classification, Machine Learning Algorithms, NDVI, Normalized Difference Vegetation Index, Random Forest, Riparian Vegetation, River Management, Isodata Clustering**

## I. Introduction and Motivation

Riparian vegetation refers to the plants and trees that grow along the banks of rivers, streams, and other water bodies. Also known as streamside or riverbank vegetation, riparian vegetation is important for a variety of ecological, hydrological, and social reasons. Ecologically, riparian vegetation plays a vital role in maintaining biodiversity by providing habitat for a wide range of plant and animal species, including many that are threatened or endangered. These ecosystems also help to control erosion, stabilize streambanks, and improve water quality by filtering pollutants and reducing sediment runoff [1]. Additionally, riparian vegetation can help to moderate the effects of flooding by slowing the flow of water and trapping sediment [2]. Hydrologically, riparian vegetation is important for maintaining the health and integrity of river systems. The roots of riparian plants help to stabilize streambanks and reduce erosion, while the leaves and branches of these plants shade the water and help to keep it cool [3]. Socially, riparian vegetation plays a vital role in providing recreational opportunities, such as fishing and hiking [4], and can also have economic benefits, such as providing timber and other resources [5]. However, these ecosystems are facing many threats, including urbanization, agriculture, mining, and water withdrawals. Thus, it is essential to have accurate classification and mapping of riparian vegetation to better understand these systems' distribution, health, and change dynamics. This information can be used to develop conservation and river management strategies that will help to protect and restore these valuable ecosystems, optimizing ecological, hydrological, social, and economic benefits and minimizing the costs of implementation of interventions.

Traditional methods of mapping riparian vegetation, such as field surveys, can be time-consuming, costly, and not as accurate as other methods. In-situ surveys, for instance, require trained personnel to physically visit the site, which can be difficult in remote or inaccessible areas. In contrast, aerial photography (especially orthoimages) or satellite imagery is an effective method for monitoring large areas of riparian vegetation [6]. This method can provide a broad overview of the distribution and condition of vegetation, can be used to track changes over time, and can be performed with

This work has received funding from the EU Horizon 2020 research innovation programme under GA no. 818194, from Horizon Europe under GA no. 101060179, and from the Tuscany Region under "Finanziamenti per l'alta formazione con l'attivazione di assegni di ricerca 2021 - progetto ECUSTODY CUP I53D21002420008".
Corresponding author: N. Fiorentini nicholas.fiorentini@ing.unipi.it

different equipment, such as Unmanned Aerial Vehicles, Light Detection and Ranging (LIDAR), or satellite imagery [7]. Aerial products can be used to map the extent of vegetation in large areas, identify areas of high or low vegetation density, and detect changes in vegetation cover. Nonetheless, by using the orthoimages solely, the analyst must carry out a manual classification and mapping, facing significant costs in terms of time and effort.

Artificial intelligence, particularly Machine Learning Algorithms (MLAs), could solve this task and bring significant benefits to the managing body. These algorithms use statistical techniques to analyze data and find hidden patterns within them. MLAs can be trained to recognize specific vegetation types and can be used to classify large amounts of data quickly and accurately. This can reduce the need for human interpretation and observer bias. Several research addressing this issue can be found in the literature. MLAs generally exploit multispectral or hyperspectral data as input features, and attempt to predict some riparian vegetation classes. Scholars generally exploit supervised MLAs, which implies having a ground truth to be exploited for evaluating the algorithms [8]–[12]. Unsupervised MLAs are less studied in riparian vegetation mapping as they are considered less accurate than supervised approaches [13], [14]. On the other hand, unsupervised classification does not require either annotated data or training of the MLAs, thus providing benefits in terms of implementation costs. Accordingly, we aim to further explore the field of unsupervised learning in riparian vegetation mapping in comparison with supervised solutions. To the best of our knowledge, only Townsend [15] studied unsupervised MLAs, proposing a fuzzy approach to predict riparian vegetation.

The proposed procedure aims to support the river authorities of the Tuscany Region, central Italy, which have to manage rivers, streams, and channels in an area extended for more than 22,900 km$^2$. The leading objective of this research is to verify which MLAs are better in terms of predictive performance and in terms of operations for technicians, even for those with less experience in ML modeling. We emphasize the benefits and limitations of supervised and unsupervised learning, also demonstrating that, in the framework of our research, unsupervised learning outperforms supervised one. Specifically, we propose a comparison between the unsupervised Isodata Clustering (ISO Cluster) and the supervised Random Forest (RF) algorithm.

Outcomes have a significant double value. From the analytical side, results demonstrate that unsupervised algorithms can be used to classify and map riparian vegetation with a high level of reliability and accuracy, comparable with those of supervised algorithms. Furthermore, from a practical point of view, unsupervised learning permits users not to have ground truth data and, therefore, allows for avoiding expensive manual mappings on orthophotos to produce a training dataset. This process also bypasses the inherent error due to the experience and the capability of the human operator in determining the training set needed for supervised learning.

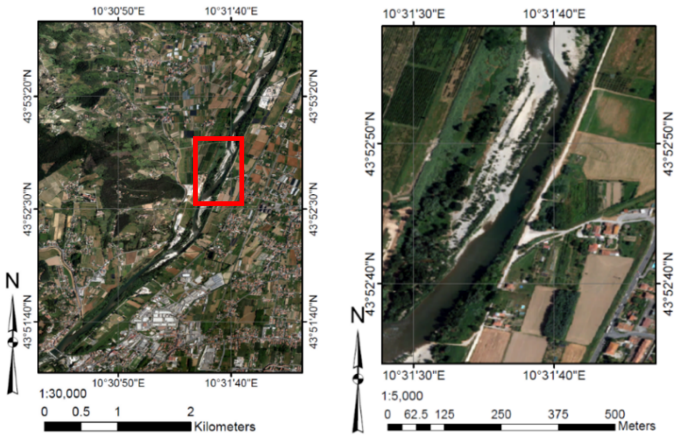


(a) (b)

Fig. 1: The Serchio River, Tuscany (Italy) (a) and the study area (b)

## II. Data

### A. Study area

The extension of the study area is 1.37 km$^2$, i.e., 1,323,138 pixels. The study area extension refers to a buffer of 150 m (75 meters per side) made along the Serchio River (Fig. 1a), in the Tuscany region, central Italy. Figure 1b corresponds to the area within the red rectangle in Fig. 1a so to show the details of the high-resolution orthoimage in use, such as the buildings and the unpaved gravel roads along the Serchio River. Fig. 1b is the reference for the qualitative assessment of MLAs that we discuss in Section IV.

### B. Input feature and output classes definition

The MLAs calibrated in the present research use as input features the Normalized Difference Vegetation Index (NDVI), i.e., a vegetation index that uses the reflectance of light in the red and Near Infrared (NIR) wavelengths to determine the health and density of vegetation [16]. NDVI values range from -1 to 1, with higher values indicating denser and healthier vegetation, and lower values indicating less vegetation or vegetation in poor condition. NDVI is commonly used in remote sensing and GIS applications to map and monitor vegetation growth and change over time. NDVI can be computed as in (1):

$$NDVI = \frac{NIR - RED}{NIR + RED} \tag{1}$$

where NIR is the reflectance of light in the near-infrared wavelength, and RED is the reflectance of light in the red wavelength. Healthy vegetation typically has NDVI values between 0.4 and 0.8, while values between 0.1 and 0.4 indicate bare soil or urban areas. NDVI values lower than 0.1 can indicate the presence of water or other non-vegetation features. Output classes of MLAs have been defined according to the domain knowledge of the authors; they are five, namely "Water", "Bare Soil", "Grass", "Shrubs", and "Trees".

TABLE I: HYPERPARAMETERS OF MLAs

| Hyperparameter | Value |
|---|---|
| Max Number of Trees (RF) | 50 |
| Max Tree Depth (RF) | 30 |
| Max Number of Samples per Class (RF) | 1000 |
| Number of classes (ISO Cluster) | 5 |
| Minimum Class Size (ISO Cluster) | 20 |
| Sample Interval (ISO Cluster) | 10 |

TABLE II: TRAINING SET DATA FOR RANDOM FOREST

| Class | Pixels | Area [$m^2$] | % of the total |
|---|---|---|---|
| Water | 54,431 | 56,507 | 4.12% |
| Bare Soil | 35,195 | 36,538 | 2.67% |
| Grass | 23,633 | 24,534 | 1.79% |
| Shrubs | 8,913 | 9,253 | 0.68% |
| Trees | 35,615 | 36,974 | 2.70% |
| **Total** | **157,787** | **163,806** | **11.96%** |

### C. Hyperparameters of MLAs, training, and test

In order to calibrate MLAs, some hyperparameters have to be defined before the training phase. Table I reports the list of selected hyperparameters for both RF and ISO Cluster.

The RF algorithm needs a training dataset since it is a supervised MLA. Accordingly, we manually defined a training set (i.e., a ground truth) in GIS environment[1]. Compared to the study area, the training set corresponds to a percentage of 11.96%. Table II provides details of the training set, in terms of extent in pixels, $m^2$, and as a percentage of the total. As regards the ISO Cluster, five potential clusters were considered; in this way, it is also possible to make direct comparisons with the classification in five possible classes made by the RF.

As regards the evaluation of the MLAs (test phase), an additional polygon-based layer has been defined in a GIS environment (i.e., a second ground truth) which allows for verifying the performance of both models. The polygons of this layer do not overlap those of the training set, in order to have total inequality between training data and test data. Table II provides all the details of the test set, in terms of extent in pixels, $m^2$, and as a percentage of the total. It can be seen that the test set covers an area equal to 3.88% of the study area. The remaining percentage of the study area was used to make predictions with the MLAs. This area does not belong to either the training or test set.

[1]ArcGIS Desktop: Release 10.5

TABLE III: TEST SET DATA

| Class | Pixels | Area [$m^2$] | % of the total |
|---|---|---|---|
| Water | 21538 | 22360 | 1.63% |
| Bare Soil | 6218 | 6455 | 0.47% |
| Grass | 5174 | 5371 | 0.39% |
| Shrubs | 5358 | 5562 | 0.41% |
| Trees | 12851 | 13341 | 0.97% |
| **Total** | **51139** | **53090** | **3.88%** |

## III. Methodology

### A. Machine Learning Algorithms

Two different categories of MLAs have been exploited in the present research: an unsupervised and a supervised MLA. The Isodata Clustering [17], or ISO Cluster, that has been used in the present research, is an unsupervised clustering algorithm developed in the 1970s. It is designed to address some of the limitations of the original K-means algorithm, particularly when dealing with large datasets. For instance, selecting the right number of clusters (K) in K-means can be challenging. ISO cluster may offer improvements in automatically determining the optimal number of clusters, reducing the need for manual selection or grid search. Moreover, K-means is sensitive to outliers, which can disproportionately influence the position of cluster centroids. ISO cluster may incorporate mechanisms to handle outliers more robustly, making the algorithm less susceptible to their influence.

The algorithm starts by randomly selecting a set of initial cluster centroids, then it iteratively re-assigns data points to the closest centroid and re-computes the cluster centroids based on the new assignment of points. The main difference between ISO Cluster and K-means is that the former also includes an additional step of splitting or merging clusters based on certain criteria, such as cluster size and standard deviation of the data points in the cluster. The process is repeated until the cluster assignments no longer change. ISO Cluster can be used for both continuous and categorical data.

Conversely, RF [18] is an ensemble supervised machine learning algorithm that combines multiple decision trees (i.e., Classification and Regression Trees, CARTs) to make a prediction. By exploiting a bootstrap aggregation and feature randomness process, RF randomly selects a subset of features to split on at each decision node and generates several uncorrelated CARTs. The final prediction is made by combining the predictions of all individual CARTs, by voting for the majority of predicted class. Compared to a single CART, the RF algorithm should be less prone to the overfitting issue, generally resulting in improved accuracy.

### B. Performance metrics

MLAs have been evaluated according to the set of performance metrics reported below (2)- (7). $F_1$ stands for F1-Score, whereas $\kappa$ stands for Cohen's Kappa Index [19]. Finally, FM represents the Fowlkes–Mallows Index [20].

$$Precision = \frac{TP}{TP + FP} \tag{2}$$

$$Recall = \frac{TP}{TP + FN} \tag{3}$$

$$Accuracy = \frac{TP + TN}{TP + TN + FN + FP} \tag{4}$$

$$F_1 = \frac{2 * Precision * Recall}{(Precision + Recall)} \tag{5}$$

$$\kappa = \frac{p_0 - p_e}{1 - p_e} \tag{6}$$

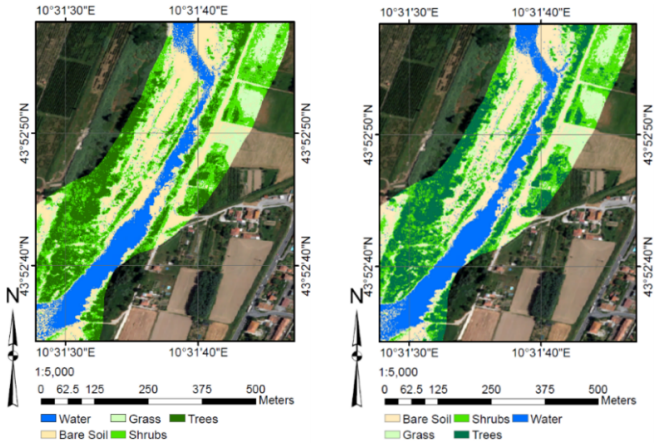


(a) (b)

Fig. 2: Random Forest (a) and Isodata Clustering (b)

$$FM = \sqrt{Precision * Recall)} \tag{7}$$

where TP is the number of True Positive samples, TN is the number of True Negative samples, FP is the number of False Positive samples, FN is the number of False Negative samples, $p_0$ is the observed proportional agreement between actual and predicted values, and $p_e$ is the probability that true values and false values agree by chance.

All the above-mentioned performance metrics can be derived from the so-called Confusion Matrix, i.e., an n-by-n table (where n is the number of classes) that summarizes the number of correct and incorrect predictions made by a model, highlighting errors in the identification of the classes. It is essential to have as many metrics as possible, as each of them highlights a particular aspect of the classifier, hiding others.

## IV. Results and Discussion

Fig. 2 below shows the classification maps performed by MLAs. The reference RGB image is in Fig. 1b. It is possible to visually and qualitatively compare their predictions. We propose an enlargement of the study area in order to perceive the granularity of them. Considering that orthoimages have been employed as input products, we can also directly measure the extension of areas belonging to different classes. This will be essential for river management bodies, as it allows for planning maintenance interventions and estimating their cost precisely and reliably. From Fig. 2, we can observe that MLAs behave similarly and provide similar outcomes regarding the prediction of riparian vegetation classes. It seems that the ISO Cluster (Fig. 2b) produces less noise than RF (Fig. 2a) when mapping "Water", and that it is able to better perceive the distinction between the latter and "Bare Soil"; it is worth noting the visual difference between the mapping of the two classifiers in the left lower corner (according to Figure 1b, there should be water, even if it is possible to perceive the underneath bare riverbed).

The quantification of the predictive performance of MLAs on the test area was performed by defining a layer composed of 50,000 points overlaying the test polygons; such evaluation points are then associated with the ground truth values belonging to the test polygons and the prediction values of the MLAs. The points are randomly generated within the test polygons and stratified, i.e., they are randomly distributed within each class, with each class having a number of points proportional to its relative area. Subsequently, Confusion Matrices can be computed (Table IV and Table V).

TABLE IV: CONFUSION MATRIX (TEST PHASE) FOR RF

| Class | Water | Bare Soil | Grass | Shrubs | Trees | Total |
|---|---|---|---|---|---|---|
| **Water** | **20740** | 87 | 0 | 0 | 0 | 20827 |
| **Bare Soil** | 319 | **5857** | 192 | 0 | 9 | 6377 |
| **Grass** | 0 | 135 | **4179** | 177 | 23 | 4514 |
| **Shrubs** | 0 | 0 | 688 | **4957** | 1204 | 6849 |
| **Trees** | 0 | 0 | 0 | 105 | **11328** | 11433 |
| **Total** | 21059 | 6079 | 5059 | 5239 | 12564 | 50000 |

TABLE V: CONFUSION MATRIX FOR ISODATA CLUSTERING

| Class | Water | Bare Soil | Grass | Shrubs | Trees | Total |
|---|---|---|---|---|---|---|
| **Water** | **21033** | 263 | 2 | 0 | 4 | 21302 |
| **Bare Soil** | 26 | **5678** | 180 | 0 | 5 | 5889 |
| **Grass** | 0 | 138 | **4213** | 180 | 23 | 4554 |
| **Shrubs** | 0 | 0 | 664 | **4884** | 964 | 6512 |
| **Trees** | 0 | 0 | 0 | 175 | **11568** | 11743 |
| **Total** | 21059 | 6079 | 5059 | 5239 | 12564 | 50000 |

Tables IV and V highlight that the MLAs work adequately, generally assigning the correct class to the test pixels. This is confirmed since most of the samples are located on the major diagonal of the Confusion Matrix, i.e., they are TP or TN (samples are TP or TN depending on the class being analyzed). Points outside the major diagonal are considered FP (those below and to the left of the diagonal) or FN (those above and to the right of the diagonal). To better understand the predictive performance of the classifiers, the values included in the confusion matrices can be recombined using (2)-(7). Tables VI and VII show these metrics and allow for an objective comparison of the two classifiers. In Table VI, cells with a grey background represent the highest metric among the two classifiers.

First of all, we can affirm that both models are capable of decently handling this task, since the considered metrics are, generally speaking, adequately high for the classes to be predicted. Furthermore, it can be observed that the metrics of the two MLAs are numerically similar; the $F_1$ parameter allows us to understand that the ISO Cluster slightly outperforms the

TABLE VI: PERFORMANCE METRICS FOR MLAS

| | Random Forest | | | Isodata Clustering | | |
|---|---|---|---|---|---|---|
| **Class** | **Prec.** | **Rec.** | $F_1$ | **Prec.** | **Rec.** | $F_1$ |
| Water | 0.985 | 0.996 | 0.990 | 0.999 | 0.987 | 0.993 |
| Bare Soil | 0.963 | 0.918 | 0.940 | 0.934 | 0.964 | 0.949 |
| Grass | 0.826 | 0.926 | 0.873 | 0.833 | 0.925 | 0.877 |
| Shrubs | 0.946 | 0.724 | 0.820 | 0.932 | 0.750 | 0.831 |
| Trees | 0.902 | 0.991 | 0.944 | 0.921 | 0.985 | 0.952 |
| **Weighted Average** | **0.943** | **0.941** | **0.939** | **0.949** | **0.948** | **0.946** |

TABLE VII: AGGREGATE EVALUATION METRICS OF MLAS

| MLA | Accuracy | $\kappa$ | FM |
|---|---|---|---|
| Random Forest | 0.941 | 0.919 | 0.942 |
| Isodata Clustering | 0.948 | 0.928 | 0.948 |

RF. As mentioned, this MLA does not require a training set to be created manually, thus saving time, money, and avoiding possible human errors during the creation of the ground truth. We can also appreciate that the weighted average metrics, i.e., the metrics averaged over all classes and weighted according to the number of samples belonging to each class, are higher for the ISO Cluster.

MLAs exhibit a common limit, even if not excessively significant; it lies in the non-negligible number of FPs relating to the "Grass" class (limited precision) and in that of FNs for the "Shrubs" class (limited recall). Nonetheless, it should be considered that the process of distinguishing these two classes on the basis of the NDVI is a complex activity even for a human operator since the values assumed by this parameter are basically similar. Therefore, considering the outcomes, we can confirm that the MLAs behave no worse than a human would do manually.

Table VII is proof of the formerly discussed outcomes, showing how the aggregate evaluation metrics of the two classifiers are markedly high, also confirming that the ISO Cluster slightly outperforms the RF classifier.

## V. Discussion and Conclusions

In the present paper, we proposed a cost-effective and efficient solution for mapping riparian vegetation of rivers by using MLAs. To classify the riparian vegetation detected in high-resolution aerial orthoimages, we calibrated an unsupervised ISO Cluster and a supervised RF, exploiting the NDVI as an input feature. We found that the Isodata Clustering algorithm slightly outperformed the Random Forest, making it a suitable operating tool for addressing this task.

It is worth noting that some limitations may arise when using MLAs to classify riparian vegetation. Firstly, a limited training dataset (for RF only): vegetation may vary greatly depending on location, season, and other factors, making it difficult to collect a large and diverse set of training samples. Secondly, a high intra-class variability: even within a single class of vegetation (e.g. "Trees"), there can be significant variations in shape, color, and species. This can make it difficult for an MLA to accurately classify all samples of that class. Thirdly, the interference from other environmental factors: lighting, weather, and the presence of other objects (e.g. buildings, roads) may interfere with the appearance of vegetation, making it difficult for an MLA to classify it accurately. Fourthly, the class imbalance issue: data for some vegetation classes are more limited than for other classes, making it difficult for an MLA to accurately classify the under-represented classes. Fifthly, the predictions of MLAs can be affected by the inherent limitations of the input feature. Indeed, NDVI suffers from surface shading. In the areas along the banks of the Serchio river, where there are trees whose foliage gives shade to the water, the NDVI takes on higher values than in unshaded water. In such areas, therefore, MLAs could predict the "Bare Soil" class instead of "Water". This limitation could be overcome by using a greater number of input features, including for example also the RGB bands or a combination thereof, aimed at a better identification of the water and the other classes. Additionally, further vegetation-related indexes can be used, such as green NDVI (gNDVI) [21], [22], soil-adjusted vegetation index (SAVI) [22], and the normalized difference red edge (NDRE) [22], [23], or a combination of them.

Finally, there is a limit in evaluating the accuracy of MLAs across "borderline" areas, i.e., in those areas where there is a separation between one class and another. In these areas, there would be significant difficulties in recognizing the correct classes even for a human operator. Therefore, at the moment, we cannot evaluate the performance of MLAs in such areas. Presumably, this issue can be reduced by exploiting images with a higher resolution; one should be able to define reliable test polygons even in borderline areas and evaluate MLAs within them. This task will constitute future research that we intend to pursue, as well as to exploit a larger test dataset to provide more precise and general insights into MLAs' performance. Additionally, a comparison with state-of-the-art algorithms would lead to a more transparent and objective assessment.

Nonetheless, our proposed methodology offers many benefits, such as easy calibration, fast training, adequate reliability, and low implementation cost. The proposed methodology should facilitate river management practices that can lead to a more sustainable and healthier environment for both rivers and the surrounding communities. Identifying riparian vegetation automatically can improve maintenance planning of managing bodies. When specific types of vegetation in an area are detected, it is possible to estimate accurately when certain plants are likely to overgrow and require maintenance cuts. This knowledge helps to avoid unnecessary in-situ inspections. Additionally, if vegetation can be accurately detected using aerial ortho-images, it is possible to bypass inspections during the initial mapping of the managed area. This is especially valuable in hard-to-reach areas that are challenging to monitor.

## Acknowledgment

The authors sincerely thank "Agenzia per le Erogazioni in Agricoltura" (AGEA) for providing orthoimages (RGB and NIR data) of the Serchio river.

## Author Contributions

Nicholas Fiorentini: Conceptualisation, Data Curation, Formal Analysis, Investigation, Methodology, Resources, Software, Validation, Visualization, Writing Original Draft, Review and Editing. Manlio Bacco: Conceptualisation, Validation, Review and Editing. Alessio Ferrari: Conceptualisation,

Validation, Review and Editing. Massimo Rovai: Conceptualisation, Data Curation, Validation, Supervision, Review and Editing. Gianluca Brunori: Conceptualisation, Supervision, Review and Editing, Project Administration, Funding Acquisition.

## REFERENCES


[1] R. J. Naiman and H. Decamps, "The ecology of interfaces: riparian zones," *Annual review of Ecology and Systematics*, vol. 28, no. 1, pp. 621–658, 1997.

[2] A. G. Garssen, A. Baattrup-Pedersen, L. A. Voesenek, J. T. Verhoeven, and M. B. Soons, "Riparian plant community responses to increased flooding: A meta-analysis," *Global Change Biology*, vol. 21, no. 8, pp. 2881–2890, 2015.

[3] E. Tabacchi, L. Lambs, H. Guilloy, A.-M. Planty-Tabacchi, E. Muller, and H. Decamps, "Impacts of riparian vegetation on hydrological processes," *Hydrological processes*, vol. 14, no. 16-17, pp. 2959–2976, 2000.

[4] M. Saklaurs, A. A. Liepiņa, D. Elferts, and Ā. Jansons, "Social perception of riparian forests," *Sustainability*, vol. 14, no. 15, p. 9302, 2022.

[5] B. D. Clinton, "Stream water responses to timber harvest: Riparian buffer width effectiveness," *Forest Ecology and Management*, vol. 261, no. 6, pp. 979–988, 2011.

[6] R. G. Congalton, K. Birch, R. Jones, and J. Schriever, "Evaluating remotely sensed techniques for mapping riparian vegetation," *Computers and Electronics in Agriculture*, vol. 37, no. 1-3, pp. 113–126, 2002.

[7] M. Rusnák, T. Goga, L. Michaleje, M. Šulc Michalková, Z. Máčka, L. Bertalan, and A. Kidová, "Remote sensing of riparian ecosystems," *Remote Sensing*, vol. 14, no. 11, p. 2645, 2022.

[8] P. E. Carbonneau, S. J. Dugdale, T. P. Breckon, J. T. Dietrich, M. A. Fonstad, H. Miyamoto, and A. S. Woodget, "Adopting deep learning methods for airborne rgb fluvial scene classification," *Remote Sensing of Environment*, vol. 251, p. 112107, 2020.

[9] G. Milani, M. Volpi, D. Tonolla, M. Doering, C. Robinson, M. Kneubühler, and M. Schaepman, "Robust quantification of riverine land cover dynamics by high-resolution remote sensing," *Remote sensing of environment*, vol. 217, pp. 491–505, 2018.

[10] E. Rommel, L. Giese, K. Fricke, F. Kathöfer, M. Heuner, T. Mölter, P. Deffert, M. Asgari, P. Näthe, F. Dzunic *et al.*, "Very high-resolution imagery and machine learning for detailed mapping of riparian vegetation and substrate types," *Remote Sensing*, vol. 14, no. 4, p. 954, 2022.

[11] M. M. Bolick, C. J. Post, E. A. Mikhailova, H. A. Zurqani, A. P. Grunwald, and E. A. Saldo, "Evaluation of riparian tree cover and shading in the chauga river watershed using lidar and deep learning land cover classification," *Remote Sensing*, vol. 13, no. 20, p. 4172, 2021.

[12] D. E. G. Furuya, J. A. F. Aguiar, N. V. Estrabis, M. M. F. Pinheiro, M. T. G. Furuya, D. R. Pereira, W. N. Gonçalves, V. Liesenberg, J. Li, J. Marcato Junior *et al.*, "A machine learning approach for mapping forest vegetation in riparian zones in an atlantic biome environment using sentinel-2 imagery," *Remote Sensing*, vol. 12, no. 24, p. 4086, 2020.

[13] K. Yoshida, S. Pan, J. Taniguchi, S. Nishiyama, T. Kojima, and M. T. Islam, "Airborne lidar-assisted deep learning methodology for riparian land cover classification using aerial photographs and its application for flood modelling," *Journal of Hydroinformatics*, vol. 24, no. 1, pp. 179–201, 2022.

[14] K. Peerbhay, O. Mutanga, R. Lottering, and R. Ismail, "Mapping solanum mauritianum plant invasions using worldview-2 imagery and unsupervised random forests," *Remote Sensing of Environment*, vol. 182, pp. 39–48, 2016.

[15] P. A. Townsend, "A quantitative fuzzy approach to assess mapped vegetation classifications for ecological applications," *Remote Sensing of Environment*, vol. 72, no. 3, pp. 253–267, 2000.

[16] F. Kriegler, W. Malila, R. Nalepka, and W. Richardson, "Preprocessing transformations and their effects on multispectral recognition," *Remote sensing of environment, VI*, p. 97, 1969.

[17] G. H. Ball and D. J. Hall, "A clustering technique for summarizing multivariate data," *Behavioral science*, vol. 12, no. 2, pp. 153–155, 1967.

[18] L. Breiman, "Random forests," *Machine learning*, vol. 45, pp. 5–32, 2001.

[19] J. Cohen, "A coefficient of agreement for nominal scales," *Educational and psychological measurement*, vol. 20, no. 1, pp. 37–46, 1960.

[20] E. B. Fowlkes and C. L. Mallows, "A method for comparing two hierarchical clusterings," *Journal of the American statistical association*, vol. 78, no. 383, pp. 553–569, 1983.

[21] H. Cicek, M. Sunohara, G. Wilkes, H. McNairn, F. Pick, E. Topp, and D. Lapen, "Using vegetation indices from satellite remote sensing to assess corn and soybean response to controlled tile drainage," *Agricultural Water Management*, vol. 98, no. 2, pp. 261–270, 2010.

[22] J. Jorge, M. Vallbé, and J. A. Soler, "Detection of irrigation inhomogeneities in an olive grove using the ndre vegetation index obtained from uav images," *European Journal of Remote Sensing*, vol. 52, no. 1, pp. 169–177, 2019.

[23] B. Boiarskii and H. Hasegawa, "Comparison of ndvi and ndre indices to detect differences in vegetation and chlorophyll content," *J. Mech. Contin. Math. Sci*, vol. 4, pp. 20–29, 2019.